Dalton Transactions

BODIPY-functionalized 1,10-phenanthroline as long wavelength sensitizers for near-infrared emission of ytterbium (III) ion

Journal:	*Dalton Transactions*
Manuscript ID	DT-ART-07-2019-002850.R2
Article Type:	Paper
Date Submitted by the Author:	13-Aug-2019
Complete List of Authors:	Kukoyi, Adedayo; Eastern Illinois University Micheli, Eric; Eastern Illinois University, Chemistry Liu, beibei; Eastern Illinois University He, Hongshan; Eastern Illinois University, Chemistry May, P.; South Dakota State University College of Education and Human Sciences, Physical Chemistry Department of Chemistry

Journal Name

ARTICLE

BODIPY-functionalized 1,10-phenanthroline as long wavelength sensitizers for near-infrared emission of ytterbium (III) ion

Adedayo Kukoyi, [a] Eric A. Micheli,[a] Beibei Liu,[a] Hongshan He,*[a] and P. Stanley May [b]

Received 00th January 20xx,
Accepted 00th January 20xx

DOI: 10.1039/x0xx00000x

www.rsc.org/

Two BODIPY (4,4-difluoro-4-bora-3a,4a-diaza-s-indacene) moieties were chemically appended to the 4,7-positions of 1,10-phenanhtroline resulting in two new ligands (BODIPY-Phen and 4I-BODIPY-Phen) with strong absorption at 507 nm and 540 nm, respectively. BODIPY-Phen emits strongly centered at 507 nm, whereas the fluorescence of 4I-BODIPY-Phen was completely quenched due to the introduction of four I atoms at its 2,6 positions. Two ligands reacted readily with tris(1,1,1,5,5,5-hexafluoro-2,4-pentanedionate) ytterbium (III) dihydrate through substitution reactions forming eight-coordinate complexes that emits strongly at 976 nm upon excitation at their absorption maximal positions. Both complexes exhibited a lifetime of ~ 11 μs in dichloromethane at room temperature.

Introduction

The fluorescence-based diagnosis has emerged as a powerful tool for gaining a greater understanding of structural and functional properties in living systems.[1, 2] The information provided is crucial to the visualization of biological events, development of new medicines, and assessment of the effectiveness of medical treatments.[3-5] The key to the diagnosis is the sensitivity of the probe. Currently available clinical probes emit in the visible region and their fluorescence spectra overlap with autofluorescence from substrates, which significantly limits test sensitivity.[5, 6] Most state-of-the-the-art probes also require excitation at a short wavelength, which often results in severe photobleaching of biological substrates. Therefore, it is desirable to develop novel fluorescent probes that emit strongly in the near-infrared (NIR) region under long wavelengths excitation. NIR probes will not only increase sensitivity by eliminating background signals but also provide deep penetration capability for *in vivo* imaging. Certain lanthanide ions are potential NIR probes.[7-10] For example, ytterbium (III) displays emission at 980 nm, which is usually realized by a sensitization process (the "antenna effect"). In this process, energy from the excited state (usually a triplet state) of a sensitizer transfers to the excited state of Yb(III) ion. After relaxation to its ground state, NIR emission is produced.[11-13]

Two challenges have to be addressed in regards to biological applications of NIR emitting lanthanide complexes. The first one is to suppress the fluorescence quenching from vibrations of X-H (X = N, O, C) in the vicinity of the coordination sphere, which can be partially overcome by the formation of complexes with high coordination numbers.[13-19] This provides a barrier for the access of solvent molecules to the central lanthanide ion. The second challenge is to broaden the absorption window of ligands toward the red light region.[7] This will enable the use of long wavelength light sources to reduce the photodegradation, which is significant when a UV or a near UV light source is used. This can be addressed by appending chromophore to a ligand-binding-group (LBG). During the last two decades, numerous attempts have been made and promising results have been obtained.[13] Among all lanthanide ions, ytterbium (III) exhibits the strongest emission in the NIR region; therefore is a potential candidate for diagnostic applications. However, it is quite challenging to sensitize the Yb (III) ion under long wavelength excitation due to the weak absorption of the ligands that are normally used to form coordination compounds.

BODIPY dyes have been explored as potential sensitizers for Yb(III)-centered NIR emission. BODIPY, abbreviated from 4,4-difluoro-4-bora-3a,4a-diaza-s-indacene, is a family of boron-dipyrromethene compounds that have high absorptivity and tunable spectral characteristics in the visible region.[20-25] Though the BODIPY core lacks the binding capability to the Yb(III) ion, it can be modified by a lanthanide-binding-group (LBG) to bring the BODIPY close to Yb(III) for sensitizing.[26] In 2006, Jean-Claude G. Bünzli et al[27] linked a terpyridine to a BODIPY core and prepared its Yb(III) complex, which emitted moderately at 980 nm. We attached an 8-hydroxyquinoline to a BODIPY core and found the resulting Yb(III) complex also emitted at 980 nm upon excitation at 507 nm.[28, 29] Its iodinated analog sensitizes effectively with a much longer lifetime upon excitation at 535 nm.[28] The enhancement is attributed to an efficient intersystem crossing for a higher triplet yield due to a "heavy atom" effect. Recently, we linked two BODIPY moieties to 1,10-phenanthroline and found it can sensitize the ytterbium emission after the coordination to the metal.[30] To further our work in this direction, we designed two new BODIPY-modified 1,10-

[a] Department of Chemistry and Biochemistry, Eastern Illinois University, Charleston, IL 61920 Email: hhe@eiu.edu. Tel: 1-217-581-6231
[b] Department of Chemistry, University of South Dakota, Vermillion, SD 57069.
† Footnotes relating to the title and/or authors should appear here.
Electronic Supplementary Information (ESI) available: [details of any supplementary information available should be included here]. See DOI: 10.1039/x0xx00000x

phenanthroline ligands and their interaction with tris(1,1,1,5,5,5-hexafluoro-2,4-pentanedionate) ytterbium (III) dihydrate, $[Yb(HFA)_3(H_2O)_2]$ as shown in **Scheme 1**. The resulting complexes are eight-coordinate with strong NIR emission in the near-infrared region. In this report, the synthesis, characterization of ligands and their interactions with ytterbium (III) will be discussed.

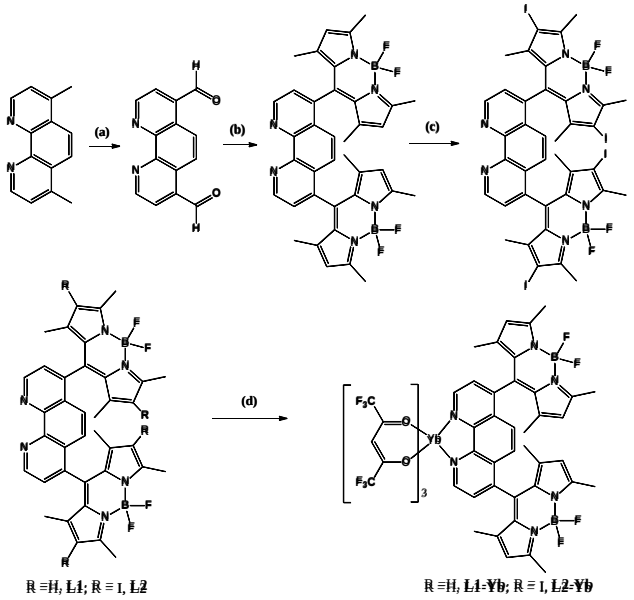

Scheme 1 Synthesis of BODIPY-modified 1,10-phenanthroline ligands and their ytterbium (Ⅲ) complexes. (a) SeO_2, dioxane, reflux; (b), CH_2Cl_2, N_2, TFA; DDQ; Et_3N; BF_3OEt_2; (c) I_2, HIO_3, EtOH; (d) $[(HFA)_3Yb(H_2O)_2]$, toluene, r.t.

Experimental Section

Reagent and General procedures

4,7-dimethyl-1,10-phenanthroline (4,7-Me-Phen), SeO_2, $BF_3{\cdot}OEt_2$ (48%), HIO_3, I_2, 2,3-dichloro-5,6-dicyano-1,4-benzoquinone (DDQ), 2,4-dimethylpyrrole and triethylamine (Et_3N) were obtained commercially and used without further purification. Tris(1,1,1,5,5,5-hexafluoro-2,4-pentanedionate) ytterbium (III) dihydrate ($[(HFA)_3Yb(H_2O)_2]$) was purchased from the Strem Chemicals, Inc. and was used directly for reactions. Solvents for photophysical studies were ACS grade and ultra-dry in Aeroseal container and used as received. $CDCl_3$ was from the Cambridge Isotope Laboratories with 99.8% D in ampule and used without further purification. Elemental compositions were determined on a Perkin Elmer Series II-2400 CHNS analyser. All other chemicals and solvents for synthesis and purification were analytical grade and used as received. 4,7-diformyl-1,10-phenathroline was prepared according to the literature method[31] and confirmed by the ^1H NMR and MS (Figure S1 –S4).

Synthesis of L1

To a dry dichloromethane (150 mL) solution of 4,7-diformyl-1,10-phenanthroline (346 mg, 2 mmol) was added 2, 4-dimethylpyrrole (0.462 ml, 4 mmol) under nitrogen. A drop of $BF_3{\cdot}OEt_2$ (~ 0.05 mL) was added and the resulting solution was stirred magnetically at room temperature for 12h. To this solution 2,3-dichloro-5,6-dicyanobenzoquinone (DDQ) (0.45 g, 2 mmol) was added. After stirring for 2h, triethylamine (4 mL) and $BF_3{\cdot}OEt_2$ (4 mL) were added sequentially. The solution became fluorescent immediately under a UV lamp, indicating the formation of the final product. The solution was magnetically stirred for another 6h and the solvent was removed on a rotary evaporator. The residue was re-dissolved in about 5 mL of dichloromethane and was then loaded on column (silica) chromatography and eluted with chloroform. The major band was collected. Yield: 1.05 g, 77%. Anal Found (Calcd.) for $C_{38}H_{34}B_2F_4N_6{\cdot}CH_3OH{\cdot}H_2O$: C, 65.03 (64.84); H, 5.20 (5.58); N, 11.99 (11.63). ^1H NMR ($CDCl_3$, ppm) 9.34 (s, 2H), 7.82 (s, 2H), 7.66 (d, 2H), 5.95 (s, 4H), 2.56 (s, 12H), 1.06 (s, 12H). ESI-HR MS: 673.3055 (M+H) (calcd. 673.3045)

Synthesis of L2.

To **L1** (0.473 g, 2.0 mmol) in absolute ethanol was added I_2 (1.06 g, 10 mmol). Then HIO_3 (1.4 g, 8.0 mmol) in water (1.0 mL) was added slowly during 10 minutes. The temperature of the solution was then increased to 60˚C and the solution was stirred magnetically for 2h. During the course of the reaction, the fluorescence weakened gradually. After the completion of the reaction, the solvent was removed on a rotary evaporator. The crude product was dissolved in chloroform and purified on a silica column using chloroform as the elute. The major band was collected. The final product was crystallized from $CHCl_3$/MeOH (v/v: 1:20). Yield: 0.66 g, 80 %. Anal Found (Calcd.) for $C_{38}H_{30}B_2F_4I_4N_6$: C, 38.51 (38.81); H, 2.99 (2.57); N, 6.98 (7.15). ^1H NMR ($CDCl_3$, ppm). 9.39 (d, 2H), 7.78 (s, 2H), 7.66 (d, 2H), 2.65 (s, 12H), 1.08 (s, 12H). ESI MS:1176.9 (M+H) (Calcd. 1176.9)

Synthesis of complexes

Two complexes, **L1-Yb** and **L2-Yb**, were prepared in a similar way and a typical one is given for **L1-Yb**. To an ethanol (25 mL) solution of $[Yb(HFA)_3(H_2O)_2]$ (18 mg, 0.022 mmol) was added **L1** (15 mg, 0.022 mmol) in dichloromethane (10 mL). The solution became reddish in colour. The resulting solution was magnetically stirred for 2h at room temperature. The solid was collected, washed with ethanol and dried at 80°C for 12h. **L1-Yb**. Yield: 27 mg, 85%. Anal Calcd. (Found) for $C_{53}H_{37}B_2F_{22}N_6O_3Yb$, C, 43.31 (43.20); H, 2.54 (2.62), N 5.73 (5.53) ESI MS: 1260.2 (M-HFA) (Calcd. 1260.2); **L2-Yb**, Yield: 37 mg, 87%. Anal Calcd. (Found) for $C_{53}H_{33}B_2F_{22}I_4N_6O_6Yb$, C, 32.31 (32.54); H 1.69 (1.87), N 4.27 (4.35). ESI MS: 1791.8 (M-HFA+CO) (Calcd.1791.9)

X-ray crystallographic analysis

Single crystals of **L1** were obtained by slow evaporation of solvent from a 1:1 (v:v) mixtures of methanol and dichloromethane at room temperature. The crystals were mounted on glass fibres for data collection. Diffraction measurements were made on a CCD-based commercial X-ray diffractometer using Mo Kα radiation (λ= 0.71073 Å). The frames were collected at 125K with a scan width 0.3° in ω and integrated with Bruker SAINT Software package using narrow-frame integration algorithm. The unit cell was determined and refined by least squares upon the refinement of XYZ-centroids

of reflections above 20σ(I). The data were corrected for absorption using the SADABS program.[32] The structures were refined on F^2 using the Bruker SHELXTL (version 5.1) software package.[33] Crystal data for **L1**: $C_{40}H_{42}B_2F_4N_6O_2$, *MW* = 736.42, triclinic, space group = P-1, *a* = 8.5972(5), *b* =10.6737(6), *c* = 21.2322(13) Å, α = 97.6450 (10), *β* = 97.9850 (10)°, γ = 105.6490 (10), *V* = 1828.00 (19) Å^3, *Z* = 2, $\rho_{calcd.}$ = 1.338 Mgm^{-3}, μ(Mo-*K*α) = 0.097 mm^{-1}, *F*(000) = 772, *T* = 100 (2) K. 18013 reflections were measured, of which 6419 were unique (*R*int = 0.0345). Final *R*1 = 0.0524 and *wR*^{2} = 0.1344 values were obtained for 4724 observed reflections with $I>2\sigma(I)$, 500 parameters, and GOF = 1.023. CCDC1861312.

Photophysical measurements

Absorption spectra were obtained on a Cary500 UV-visible spectrophotometer at room temperature. Steady-state and time-resolved spectroscopy studies were performed on an FS5 fluorimeter (Edinburg Instruments) with a Xenon arc lamp as a light source. For the visible emission measurements, the slit width for emission and excitation arms was 1 nm. For the NIR emission, the slit width for both emission and excitation was 8 nm. The fluorescence quantum yield, Φ, in the visible region was measured using the following equation:

$$\Phi x = \emptyset_{ST}\left[\frac{Grad_X}{Grad_{ST}}\right]\left[\frac{n_X}{n_{ST}}\right]^2$$

where *Grad* the gradient from the plot of integrated fluorescence intensity *vs* absorbance of five samples with different concentrations, and *n* is the refractive index of the solvents. Rhodamine 6G in ethanol (Φ_{ST} = 0.95, λ_{ex} = 480 nm) was used as a reference. The decay curves of the samples were also measured on the FS5 (Edinburg Instruments) spectrometer. A laser diode EPL 375 (Edinburg Instruments) with the wavelength of 375 nm was used as light source. The NIR decay curves were acquired using an optical parametric oscillator (OPOTEK Opolette) as an excitation source. NIR emission was detected using a 0.3 m flat-field monochromator (Jobin Yvon TRIAX 320) equipped with a NIR-sensitive photomultiplier tube (Hamamatsu R2658P) in a cooled housing (Products for Research). All spectra were corrected for instrument response. The output from the photomultiplier was pre-amplified (Stanford Research SR 445A) and fed to a multichannel scaler (Stanford Research SR 430) for time-resolved photon counting. The entire system was PC controlled using LabView software.

Theoretical calculation

Calculations for ligands were performed at a density functional theory (DFT) level using Gaussian 09 software.[34] The initial input structures were built based upon the crystal structure of a similar complex. The ground state geometries of compounds were optimized using 6-31G(d) as a basis set for C, H, N, B, and F atoms and Midix for I atom and MWB28 for Yb. All other parameters were default set. No negative frequency was found in the final optimized structures. All calculations were carried out in SMD model for mimicking the solvent effect. The calculated absorption data were analyzed by GaussSum software.[35]

Results and Discussion

Synthesis and Characterization

Ligands (**L1** and **L2**) and complexes (**L1-Yb** and **L2-Yb**) are prepared according to a procedure as outlined in **Scheme 1**. The 4,7-dicarbonyl-1,-10-phenanthroline precursor was prepared by oxidation of 4,7-dimethyl-1,10-phenanthroline with SeO_2 in 1,4-dioxane with a moderate yield.[36] The **L1** was prepared by the reaction between 4,7-dicarbonyl-1,10-phenanthroline and 2,4-dimethylpyrrole in CH_2Cl_2 under N_2 for 12h in the presence of one drop of BF_3OEt_2, followed by oxidation using 2,3-dichloro-5,6-dicyano-1,4-benzoquinoline (DDQ) and chelating to BF_2 unit in the presence of triethylamine (Et_3N) and $BF_3{\cdot}OEt_2$.[37] The resulting compound **L1** was slightly yellowish. The **L1** was then reacted with iodine and HIO_3 in ethanol at 60ºC to **L2** with ~95% yield. The **L2** was purplish. The compositions of the two compounds were confirmed by elemental analysis and ^{1}H NMR (**Figures S1- S4**). Both ligands were very soluble in $CHCl_3$ and CH_2Cl_2 and slightly soluble in CH_3OH. Samples are not soluble in water, which could be a barrier to medical diagnosis and could be overcome by introducing carboxylic groups to the BODIPY. We are currently working on this direction. The color of the **L1** solution was yellowish, whereas the **L2** solution was purplish. The structure of **L1** was further confirmed by single-crystal X-ray diffraction analysis. Its ORTEP diagram is shown in **Figure 1**. The two BODIPY units, each having a B center with a tetrahedral geometry, are almost perpendicular to the 1,10-phenanthroline plan with torsion angles 86.98 (6) and 84.77 (4), respectively. The two BODIPY units are pointing away from two nitrogen atoms (N1 and N2) of the 1,10-phenanthroline unit with a distance of 10.927Å between B1 and B2. There are two methanol molecules in each asymmetric unit, both of which form an intermolecular hydrogen-bond with N1 and N2 from the neighboring unit. The crystals of the L2 diffracted weakly, therefore no X-ray diffraction data were obtained. Synthesis of the complexes, **L1-Yb** and **L2-Yb**, was achieved by mixing one equivalent of ligands with $[Yb(HFA)_3(H_2O)_2]$ in dichloromethane. The simple replacement of two H_2O molecules by the bidentate ligands afforded the desired complexes. The complexes are soluble in most organic solvents including chloroform, dichloromethane, and toluene and are slightly soluble in methanol and hexane. The compositions of the complexes were confirmed by elemental analysis.

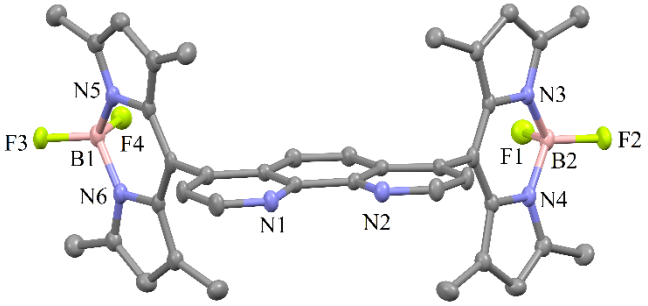

a.

Figure 1. ORTEP diagram of **L1** with 50% thermal ellipsoid probability. Hydrogen atoms and two methanol molecules were omitted for clarity.

Photophysical Properties of Ligands

Absorption and fluorescence properties of the ligands in solution at room temperature were studied. As shown in **Figure 2**, the **L1** exhibits strong absorption in the visible region with a peak position at 507 nm in CH_2Cl_2, which is quite typical for BODIPY dyes. With iodination at C2 and C6 positions in **L2**, the colour of the solution changed from yellow to pinkish and a strong absorption at 540 nm was observed, and the absorption coefficients are also enhanced. The fluorescence properties of **L1** and **L2** are different. The **L1** gives strong fluorescence at 524 nm with a quantum yield of 84.6% in CH_2Cl_2. The emission wavelength does not change too much in different solvents; however, the quantum yields vary significantly (**Table S1**) from the lowest quantum yield in DMF (8.7%) to the highest quantum yields in $CHCl_3$ (88.9%) and CH_2Cl_2 (84.6%). The **L2** emits at 569 nm with a quantum yield of about 0.4%, which is significantly lower than that of the **L1**. This is most likely due to the "heavy atom" effect from introduced iodine atoms as previously observed. The heavy atom facilitated the intersystem crossing for an increased quantum yield of triplet state, which will benefit the sensitization of near-infrared emission of ytterbium (III).

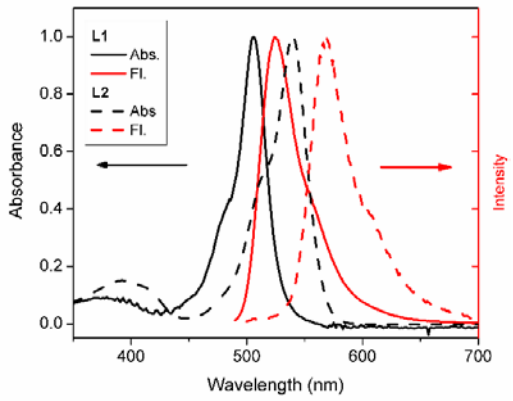

Figure 2. The normalized absorption and fluorescence of **L1** and **L2** in CH_2Cl_2 at room temperature. The concentration of the all samples is 1×10^{-6} mol/L in CH_2Cl_2.

Interaction of Ligands with Yb(III)

The interaction of ligands with Yb(III) was first examined from fluorescence titrations of $[Yb(HFA)_3(H_2O)_2]$ solutions with ligands **L1** and **L2** at room temperature. A typical spectral change of $[Yb(HFA)_3(H_2O)_2]$/**L2** system is shown in **Figure 3**. The CH_2Cl_2 solution of $[Yb(HFA)_3(H_2O)_2]$ did not give any emission between 900 and 1200 nm upon excitation at 545 nm since $[Yb(HFA)_3(H_2O)_2]$ has no absorption at 545 nm. As **L2** was added to the solution, the characteristic emission of Yb (III) in the NIR region was readily observed. The emission intensity increased with the continued addition of **L2** until the molar ratio of **L2**/Yb^{3+} reached 1.0, indicating the stoichiometric replacement of two water molecules by one **L2** ligand as shown in the following equation. Similar NIR emission changes were also observed for the **L1**/Yb^{3+} system. In addition, the reaction between L1 and $[Yb(HFA)_3(H_2O)_2]$ in $CDCl_3$ was also monitored by ^1H NMR spectroscopy as shown in **Figure S5.** The **L1** gave well-resolved peaks in $CDCl_3$ at 9.34, 7.82, and 7.89 ppm for protons on the phenanthroline fragment, and 5.95 ppm for a proton on the BODIPY ring. After different amount of $[Yb(HFA)_3(H_2O)_2]$ were added, all these peaks except those corresponding to CH_3 were broadened and shifted to low field region due to impact from paramagnetic Yb^{3+} ion. The spectrum did not change after the molar ratio was above 1.0. This result is consistent with emission spectral changes.

$$[Yb(HFA)_3(H_2O)_2] + \mathbf{L2} \rightarrow [Yb(HFA)_3(\mathbf{L2})] + 2\ H_2O$$

The isolated products showed the expected formula of $[Yb(HFA)_3(\mathbf{L1})]$ (**L1-Yb**) and $[Yb(HFA)_3(\mathbf{L2})]$ (**L2-Yb**). Their compositions were ascertained by elemental analysis. Single crystals obtained from a solution of $[Yb(HFA)_3(\mathbf{L2})]$ gave poor X-ray diffraction; therefore, no reliable structural information was obtained. However, the geometry-optimized structure of **L2-Yb**, as shown in **Figure 4**, revealed an eight-coordination geometry around Yb(III) ion. The phenanthroline unit binds to the Yb(III) through two N atoms with two BODIPY units aligned almost vertically to the phenanthroline unit with dihedral angles 87.27 and 87.60°, respectively. The Yb-O bond length varied from 2.482 to 2.526Å. The two Yb-N bond lengths are 2.700 Å and 2.690Å.

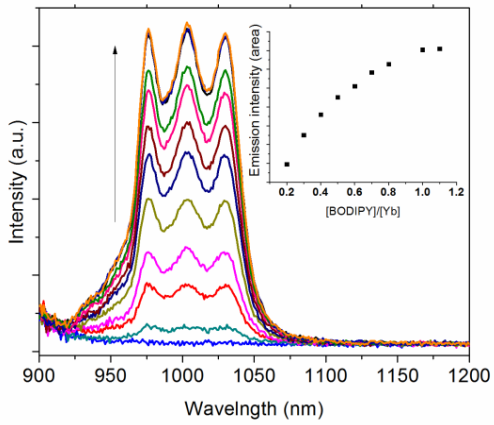

Figure 3. The increase Yb(III) emission (λ_{ex} = 545 nm) intensity of $[Yb(HFA)_3(H_2O)_2]$ in CH_2Cl_2 upon addition of **L2** at room temperature. The incubation time was five minutes after addition of L2. The concentration of $[Yb(HFA)_3(H_2O)_2]$ was 2×10^{-4} mol/L in CH_2Cl_2.

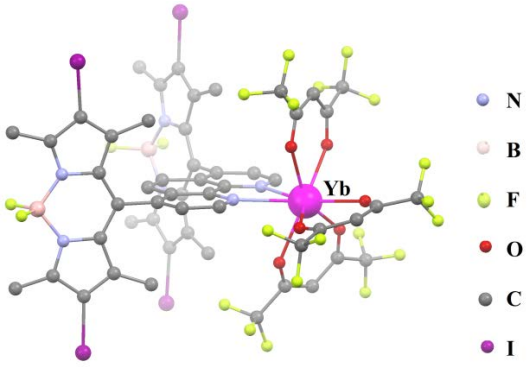

Figure 4. Side-view of geometry-optimized structure of L**2-Yb**.

Photophysical properties of the complexes

The complexes **L1-Yb** and **L2-Yb** exhibit absorption spectra in the visible region that are similar to the corresponding ligands as shown in **Figure 5**. After forming a complex, the emission wavelength shifted from 524 nm in **L1** to 550 nm in **L1-Yb** and 569 nm in **L2** to 584 nm in **L2-Yb**. The fluorescence of **L1** and **L2** decreased 95% and 15% after forming the complex with Yb(III) ion, respectively. The characteristic NIR emission spectra that are quite similar to the final spectrum during the titration are also observed. As shown in **Figure 5**, upon visible excitation, the two complexes exhibit a broad emission feature centered at 1003 nm, which contains three distinct peaks at 976, 1003 and 1019 nm, respectively. These are typical $^2F_{5/2} \rightarrow {}^2F_{7/12}$ emission peaks of the ytterbium (III) ion. The emission lifetimes of **L1-Yb** and **L2-Yb** from the exponential fitting of their decay curves at 976 nm were 11.2 and 11.3 μs, respectively. The decay curve for **L2-Yb** is also shown in **Figure 6** and **Table 1**. The calculated intrinsic quantum efficiencies Φ_{Yb} (= τ_{obs}/τ_{rad}, τ_{rad} = 1.2 ms)[38, 39] are 0.93% and 0.94%, respectively. To verify the origin of sensitization, we recorded the excitation spectra of **L1-Yb** and **L2-Yb** (λ_{em} = 976 nm). As shown in **Figure 7**, the excitation spectra match the absorption spectra very well, indicating clearly that the BODIPY moiety is responsible for the sensitization of Yb^{3+}emission.

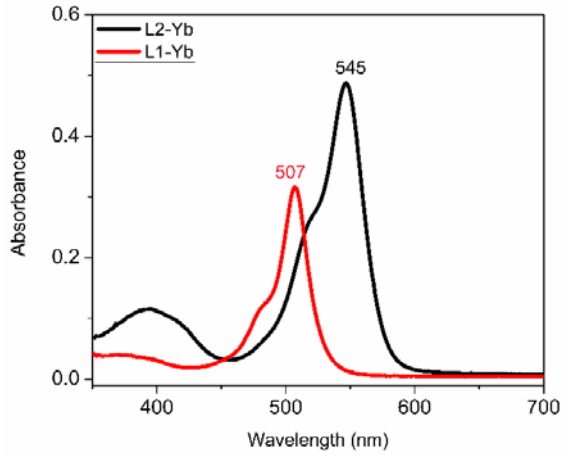

Figure 5. Absorption spectra of **L1-Yb** and **L2-Yb** in CH_2Cl_2 at room temperature. The concentration is5.18×10^{-6} mol/L.

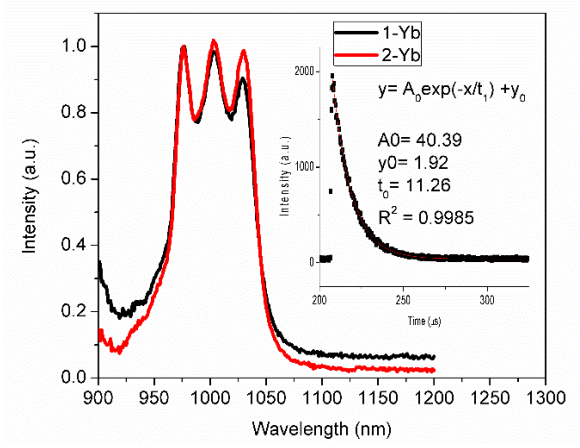

Figure 6. Normalized NIR emission spectra of **L1-Yb** (λ_{ex} = 507 nm) and **L2-Yb** (λ_{ex} = 547 nm) in CH_2Cl_2 at room temperature. The decay was monitored at 978 upon excitation at the 375 nm.

Table 1. Photophysical properties of **L1**, **L2**, **L1-Yb** and **L2-Yb** in CH_2Cl_2 at room temperature.

Compound	Abs (nm)	Emission (λ/ nm, τ)[a]	QY(%)
L1	507	524 (10 ns)	84.6[b]
L2	545	569 (<1 ns)	-
L1-Yb	507	550, 976 (11.2 μs), 1003, 1019	0.93[c]
L2-Yb	545	584, 976 (11.3 μs), 1003, 1019	0.94[c]

[a]λ_{ex} = 375 nm for the VIS emission; [b]in CH_2Cl_2; [c]calculated from Q_{Yb}= τ_{obs}/τ_{rad}, τ_{rad} = 1.2 ms

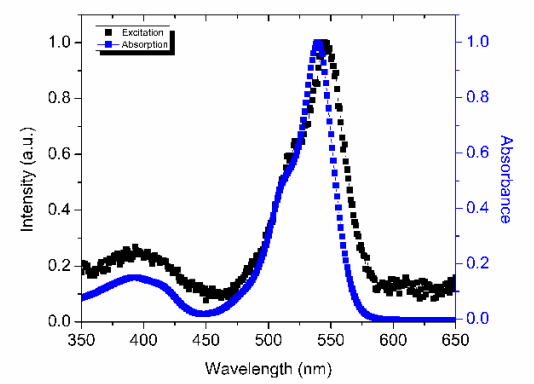

Figure 7. Excitation and absorption spectra of **L2-Yb** in CH_2Cl_2 at room temperature. The emission wavelength was 976 nm. The excitation spectrum of **L1-Yb** can be found in **Figure S6.**

The NIR emission of ytterbium (III) is sensitized by ligand-to-Yb(III) energy transfer. The energy transfer process occurs either from the triplet state of ligand to the excited state of lanthanide (III) (Dexter mechanism) or through dipole-dipole interaction (Förster mechanism).[13] An early study from Jean-Claude G. Bünzli *et al.*[26, 27] revealed that the energy level of the triplet state of BODIPY functionalized terpyridine ligand was ~ 17450 cm^{-1}, which is high enough for energy transfer to Yb(III). The sensitization was proposed to occur by a Dexter electron exchange mechanism. To probe if such a mechanism is also valid for our complexes, we added a slight excess of $[Yb(HFA)_3(H_2O)_2]$ to solutions of ligands **L1** and **L2** with the same concentration (5.18×10^{-6} M) in CH_2Cl_2 in order to generate the **L1-Yb** and **L2-Yb** and to ensure that there are no free ligands remaining in solution. The intrinsic fluorescence of ligand **L1** decreased 97%, whereas that of ligand **L2** decreased 14% (**Figures S7** and **S8**). Such a drastic decrease is a stark contrast to terpyridine and benzoic acid functionalized BODIPY-Yb complexes.[26, 27] **Figure 8** shows that the NIR emission intensities from the **L1-Yb** and **L2-Yb** solutions are very similar upon excitation at 514 nm, at which wavelength the two solutions exhibit the same absorbance. Similar emission intensities from the two solutions are also observed when the solutions are excited at their respective absorption peak positions (507 nm and 547 nm), at which the absorbance was adjusted to 0.316 (**Figure**

S9). These results demonstrate clearly that the efficient intrinsic intersystem crossing in ligand **L2,** induced by the I atoms, does not affect its ability to sensitize Yb(III) relative to ligand **L1**. Also, the fact that the sensitization efficiency is essentially identical in **L1-Yb** and **L2-Yb** would suggest that the mechanism of sensitization in both complexes is the same. The most straightforward explanation of these observations is that the Yb(III) ion can also induce near the quantitative intersystem crossing in the two complexes, after which, sensitization occurs from the triplet state of the ligand *via* a Dexter mechanism.

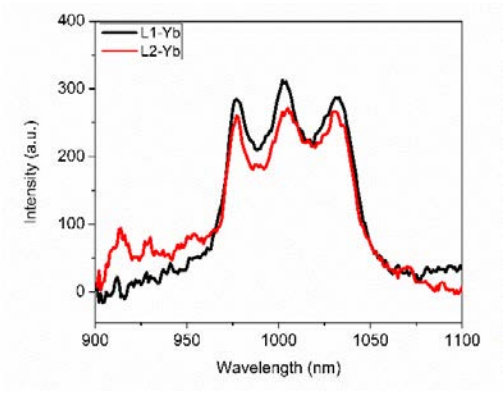

Figure 8. NIR emission spectra of **L1-Yb** and **L2-Yb** upon excitation at 514 nm. The two solutions have equal absorbance at 514 nm and show nearly equal emission intensities, indicating that the internal quantum efficiencies of sensitized emission from **1-Yb** and **2-Yb** are similar.

We performed DFT calculations for ligand **L1** and ligand **L2** and their complexes, **L1-Y** and **L2-Y**, respectively. For the free ligands, the HOMO and LUMO are both located on the BODIPY moieties (**Table S2** and **S3**). The predicted absorption spectra show a red-shift in compound **L2** relative to compound **L1**, which is consistent in trend with the measured absorption spectra. It should be mentioned that BODIPY dyes are notorious in spectral predicting due to the lack of accurate functional and bases sets for calculation.[40, 41] The triplet level for ligand L1 and L2 are respectively at 782 and 804 nm, which are quite consistent with the measured data by Zhao et al.[42] The energy levels are positioned at higher energy than the emitting energy level of Yb(III). For the complexes, the electron density at the HOMO (H) and LUMO (L) are high at BODIPY units as shown in **Figure 9**. Significant electron densities at Yb center are in L+2 and L+3, indicating the energy transfer from BODIPY to the Yb upon excitation.

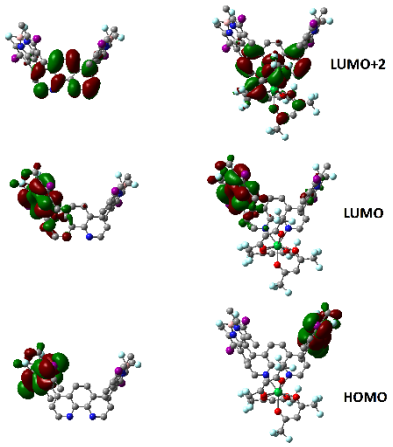

Figure 9. Electron density distribution profiles of ligand **L2** and its Yb(III) complex.

Conclusions

In conclusion, near-infrared emission of ytterbium (III) ion was sensitized successfully by an iodized BODIPY chromophore under excitation at 540 nm. Luminescence lifetimes as long as ~ 11 μs was observed for 975 nm emission in the iodinated and non-iodinated complexes. The results provide a new strategy for novel optical probes that emit in the NIR region under long wavelength excitation for sensitive biomedical imaging and detection.

Conflicts of interest

There are no conflicts to declare

Acknowledgements

HH thanks National Science Foundation (Award # 1507871) and The Extreme Science and Engineering Discovery Environment (XSEDE) (CHE130116) for financial support of this work. Authors are grateful to a crystallographer for structure refinements during the review of this article.

Notes and references

1 J. L. Sessler, W. C. Dow, D. O'Connor, A. Harriman, G. Hemmi, T. D. Mody, R. A. Miller, F. Qing, S. Springs, K. Woodburn and S. W. Young, *J. Alloys Comp.*, 1997, **249**, 146-152.

2 K. Matzumoto and J. Yuan, in *Metal Ions in Biological Systems: Vol 40: The Lanthanides and Their Interrelations with Biosystems. ed. Helmut Sigel & Astrid Sigel*, Marcel Dekker Inc., New York, 2003, vol. 40, pp. 191-226.

3 F. Leblond, S. C. Davis, P. A. Valdés and B. W. Pogue, *J. Photochem. Photobiol. B: Biology*, 2012, **98**, 77-94.

4 F. Wang, Y. Zhu, L. Zhou, L. Pan, Z. Cui, Q. Fei, S. Luo, D. Pan, Q. Huang, R. Wang, C. Zhao, H. Tian and C. Fan, *Angew. Chem. Int. Ed.*, 2015, **54**, 7349-7353.

5 M. Gao, F. Yu, C. Lv, J. Choo and L. Chen, *Chem. Soc. Rev.*, 2017, **46**, 2237-2271.

6 L. Wu and X. Qu, *Chem. Soc. Rev.*, 2015, **44**, 2963-2997.
7 H. He, *Coord. Chem. Rev.*, 2014, **273-274**, 87-99.
8 Y. Cui, B. Chen and G. Qian, *Coord. Chem. Rev.*, 2014, **273–274**, 76-86.
9 Z. Liu, W. He and Z. Guo, *Chem. Soc. Rev.*, 2013, **42**, 1568-1600.
10 J.-C. G. Bunzli, *Chem. Rev.*, 2010, **110**, 2729-2755.
11 T. Zhang, X. Zhu, C. C. W. Cheng, W.-M. Kwok, H.-L. Tam, J. Hao, D. W. J. Kwong, W.-K. Wong and K.-L. Wong, *J. Am. Chem. Soc.*, 2011, **133**, 20120-20122.
12 H. Ke, W.-K. Wong, W.-Y. Wong, H.-L. Tam, C.-T. Poon and F. Jiang, *Eur. J. Inorg. Chem.*, 2009, 1243-1247.
13 S. Comby and J.-C. G. Bünzli, in *Handbook on the Physics and Chemistry of Rare Earths*, eds. J. Karl A. Gschneidner, J.-C. G. Bünzli and V. K. Pecharsky, Elsevier, 2007, vol. 37, pp. 217-470.
14 Z. Zhang, Y. Zhou, H. Li, T. Gao and P. Yan, *Dalton Trans*, 2019, **48**, 4026-4034.
15 Q. Zhang, X. Yang, R. Deng, L. Zhou, Y. Yu and Y. Li, *Molecules*, 2019, **24**, 1253.
16 Y. Yao, H.-Y. Yin, Y. Ning, J. Wang, Y.-S. Meng, X. Huang, W. Zhang, L. Kang and J.-L. Zhang, *Inorg. Chem.*, 2019, **58**, 1806-1814.
17 H. P. Santos, E. S. Gomes, M. V. dos Santos, K. A. D'Oliveira, A. Cuin, J. S. Martins, W. G. Quirino and L. F. Marques, *Inorg. Chem. Acta*, 2019, **484**, 60-68.
18 K. Krekić, D. Klintuch, C. Lescop, G. Calvez and R. Pietschnig, *Inorg. Chem.*, 2019, **58**, 382-390.
19 Y. Ning, J. Tang, Y.-W. Liu, J. Jing, Y. Sun and J.-L. Zhang, *Chem. Sci.*, 2018, **9**, 3742-3753.
20 A. Loudet and K. Burgess, *Chem. Rev.*, 2007, **107**, 4891-4932.
21 N. Boens, V. Leen and W. Dehaen, *Chem. Soc. Rev.*, 2012, **41**, 1130-1172.
22 S. P. Singh and T. Gayathri, *Eur. J. Org. Chem.*, 2014, 4689-4707.
23 A. C. Benniston and G. Copley, *Phys. Chem. Chem. Phys.*, 2009, **11**, 4124-4131.
24 G. Ulrich, R. Ziessel and A. Harriman, *Angew. Chem. Int. Ed.*, 2008, **47**, 1184-1201.
25 C. Zhao, X. Zhang, K. Li, S. Zhu, Z. Guo, L. Zhang, F. Wang, Q. Fei, S. Luo, P. Shi, H. Tian and W.-H. Zhu, *J. Am. Chem. Soc.*, 2015, **137**, 8490-8498.
26 J. H. Ryu, Y. K. Eom, J.-C. G. Bunzli and H. K. Kim, *New J. Chem.*, 2012, **36**, 723-731.
27 R. F. Ziessel, G. Ulrich, L. Charbonnière, D. Imbert, R. Scopelliti and J.-C. G. Bünzli, *Chem. Eur. J.*, 2006, **12**, 5060-5067.
28 H. He, L. Si, Y. Zhong and M. Dubey, *Chem. Commun.*, 2012, **48**, 1886-1888.
29 Y. Zhong, L. Si, H. He and A. G. Sykes, *Dalton Trans.*, 2011, **40**, 11389-11395.
30 H. He, J. D. Bosonetta, K. A. Wheeler and S. P. May, *Chem. Comm.*, 2017, 10120--10123.
31 M. Yanagida, R. Katoh, L. P. Singh, A. Islam, M. K. Nazeeruddin, K. Sayama, H. Sugihara, a. M. Grätzel, K. Hara and H. Arakawa, *Dalton Trans.*, 2000, 2817-2822.
32 G. M. Sheldrick, in *SADABS, Empirical Absorption Correction Program; University of Göttingen, Germany*, 1997.
33 G. M. Sheldrick, in *SHELXTLTM, Reference manual, Version 5.1 Madison, WI*, 1997.
34 M. J. T. Frisch, G. W.; Schlegel, H. B.; Scuseria, G. E.; Robb, M. A.; Cheeseman, J. R.; Scalmani, G.; Barone, V.; Mennucci, B.; Petersson, G. A.; Nakatsuji, H.; Caricato, M.; Li, X.; Hratchian, H. P.; Izmaylov, A. F.; Bloino, J.; Zheng, G.; Sonnenberg, J. L.; Hada, M.; Ehara, M.; Toyota, K.; Fukuda, R.; Hasegawa, J.; Ishida, M.; Nakajima, T.; Honda, Y.; Kitao, O.; Nakai, H.; Vreven, T.; Montgomery, Jr., J. A.; Peralta, J. E.; Ogliaro, F.; Bearpark, M.; Heyd, J. J.; Brothers, E.; Kudin, K. N.; Staroverov, V. N.; Kobayashi, R.; Normand, J.; Raghavachari, K.; Rendell, A.; Burant, J. C.; Iyengar, S. S.; Tomasi, J.; Cossi, M.; Rega, N.; Millam, N. J.; Klene, M.; Knox, J. E.; Cross, J. B.; Bakken, V.; Adamo, C.; Jaramillo, J.; Gomperts, R.; Stratmann, R. E.; Yazyev, O.; Austin, A. J.; Cammi, R.; Pomelli, C.; Ochterski, J. W.; Martin, R. L.; Morokuma, K.; Zakrzewski, V. G.; Voth, G. A.; Salvador, P.; Dannenberg, J. J.; Dapprich, S.; Daniels, A. D.; Farkas, Ö.; Foresman, J. B.; Ortiz, J. V.; Cioslowski, J.; Fox, D. J., Gaussian, Inc., Wallingford CT, 2009.
35 N. M. O'Boyle, A. L. Tenderholt and K. M. Langner, *J. Comp. Chem.*, 2008, **29**, 839-845.
36 M. Yanagida, L. P. Singh, K. Sayama, K. Hara, R. Katoh, A. Islam, H. Sugihara, H. Arakawa, M. K. Nazeeruddin and M. Grätzel, *Dalton Trans*, 2000, 2817-2822.
37 A. Cui, X. Peng, J. Fan, X. Chen, Y. Wu and B. Guo, *J. Photochem. Photobiol. A: Chem.*, 2007, **186**, 85-92.
38 N. M. Shavaleev, R. Scopelliti, F. Gumy and J.-C. G. Bunzli, *Inorg. Chem*, 2009, **48**, 7937-7946.
39 A. Aebischer, F. Gumy and J.-C. G. Bunzli, *Phys. Chem. Chem. Phys.*, 2009, **11**, 1346-1353.
40 L. Zhang and J. M. Cole, *ACS Appl. Mater. Interfaces*, 2015, **7**, 3427-3455.
41 41. B. Le Guennic, O. Maury and D. Jacquemin, *Phys. Chem. Chem. Phys.*, 2012, **14**, 157-164.
42 W. Wu, H. Guo, W. Wu, S. Ji and J. Zhao, *J. Org. Chem.*, 2011, **76**, 7056-7064.

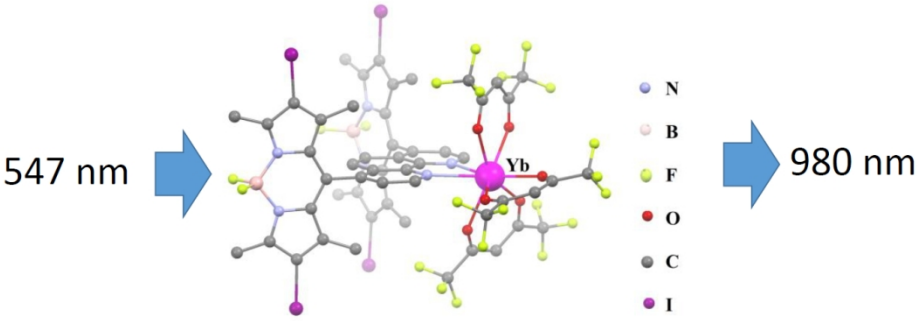

260x101mm (144 x 144 DPI)